



Ocean biology could control atmospheric $\delta^{13}\text{C}$ during glacial-interglacial cycle

Victor Brovkin and Matthias Hofmann

Potsdam Institute for Climate Impact Research, P. O. Box 601203, 14412 Potsdam, Germany (victor@pik-postdam.de; hofmann@pik-potsdam.de)

Jørgen Bendtsen

Niels Bohr Institute for Astronomy, Physics and Geophysics, Danish Center for Earth System Science, Blegdamsvej 17, DK-2100 Copenhagen, Denmark (jb@dcass.ku.dk)

Andrey Ganopolski

Potsdam Institute for Climate Impact Research, P. O. Box 601203, 14412 Potsdam, Germany (andrey@pik-postdam.de)

[1] Estimates of changes in the global carbon budget are often based on the assumption that the terrestrial biosphere controls the isotopic composition of atmospheric CO_2 since terrestrial plants discriminate against the ^{13}C isotope during photosynthesis. However, this method disregards the influence of ^{13}C fractionation by the marine biota. Here an interpretation of the glacial-interglacial shifts in the atmospheric CO_2 concentration and $\delta^{13}\text{CO}_2$ measured in the Taylor Dome ice core [Smith *et al.*, 1999] is given by accounting for possible changes in the ocean biology based on sensitivity simulations undertaken with the intermediate complexity model CLIMBER-2. With a combined scenario of enhanced biological and solubility pumps, the model simulates glacial atmospheric CO_2 and $\delta^{13}\text{CO}_2$ similar to those inferred from the ice core. The simulations reveal that a strengthening of the oceanic biological carbon pump considerably affects the atmospheric $\delta^{13}\text{CO}_2$.

Components: 8361 words, 4 figures, 2 tables.

Keywords: Biosphere; carbon cycle; CO_2 , $\delta^{13}\text{C}$; glacial-interglacial changes; modeling.

Index Terms: 0315 Atmospheric Composition and Structure: Biosphere/atmosphere interactions; 1615 Global Change: Biogeochemical processes (4805); 4815 Oceanography: Biological and Chemical: Ecosystems, structure and dynamics; 4870 Oceanography: Biological and Chemical: Stable isotopes.

Received 13 November 2001; **Revised** 9 February 2002; **Accepted** 11 February 2002; **Published** 22 May 2002.

Brovkin, V., M. Hofmann, J. Bendtsen, and A. Ganopolski, Ocean biology could control atmospheric $\delta^{13}\text{C}$ during glacial-interglacial cycle, *Geochem. Geophys. Geosyst.*, 3(5), 10.1029/2001GC000270, 2002.

1. Introduction

[2] Analysis of the global carbon-isotope budget is a powerful method for estimating carbon transfer between ocean, land, and atmosphere on decadal to

millennium timescales [see, e.g., Tans *et al.*, 1993; Bird *et al.*, 1996]. Terrestrial plants discriminate against ^{13}C during photosynthesis with averaged fractionation factor α_{LB} about -18‰ and -5‰ for C_3 and C_4 plants, respectively [Lloyd and Farqu-

har, 1994]. By contrast, ocean seawater is enriched in ^{13}C during CO_2 exchange between the sea surface and the atmosphere with an averaged fractionation factor α_O of $\sim 8.5\text{‰}$ [Siegenthaler and Münnich, 1981]. An average sample of terrestrial carbon has a relatively low $\delta^{13}\text{C}$ value of about -23‰ compared to the $\delta^{13}\text{C}_{\text{DIC}}$ of $\sim 1\text{--}2\text{‰}$ and 0‰ for ocean surface and deep waters, respectively ($\delta^{13}\text{C}_{\text{DIC}}$ is for $\delta^{13}\text{C}$ of dissolved inorganic carbon, or DIC). The gradient in $\delta^{13}\text{C}_{\text{DIC}}$ between the surface and the deep ocean is caused by the so-called biological pump [Volk and Hoffert, 1985]. Similar to terrestrial plants, marine phytoplankton discriminates ^{13}C during photosynthesis with a fractionation factor α_{MB} varying from -18‰ in the tropics to -36‰ in the polar regions [Goericke and Fry, 1994]. Decomposition of ^{13}C -depleted organic matter reduces the $\delta^{13}\text{C}_{\text{DIC}}$ values in the deep ocean and increase the $\delta^{13}\text{C}_{\text{DIC}}$ in the upper part of the water column. Ignoring the spatial and temporal variations in α_O , α_{LB} and marine productivity, the changes in the terrestrial carbon storage can be estimated from changes in the atmospheric $\delta^{13}\text{CO}_2$, or $\delta^{13}\text{C}_{\text{ATM}}$ (see appendix A, equation (A6)). Calculated in this way, $\delta^{13}\text{C}_{\text{ATM}}$ is solely controlled by changes in the terrestrial carbon storage alone.

[3] The assumptions that oceanic and terrestrial carbon storages have a constant but distinct ^{13}C fractionation factor are applied, for example, to distinguish between the oceanic and terrestrial carbon sink when trying to track the pathways of anthropogenic CO_2 [Ciais et al., 1995; Joos and Bruno, 1998; Battle et al., 2000]. However, this approach disregards changes in the biological carbon pump, which affect $\delta^{13}\text{C}_{\text{ATM}}$ as well [Tans et al., 1993]. For example, strengthening of the biological productivity leads to an increased export flux N_p that leaves surface waters enriched in ^{13}C . Consequently, the CO_2 flux across the sea surface shifts $\delta^{13}\text{C}_{\text{ATM}}$ toward higher values. The question is, how significant $\delta^{13}\text{C}_{\text{ATM}}$ is influenced by changes in the marine biota.

[4] Recently, Smith et al. [1999] published a record of the atmospheric CO_2 and $\delta^{13}\text{C}_{\text{ATM}}$ inferred from the Taylor Dome ice core for the last 26,000 years. These data constrain the reconstruction of

the global carbon isotopic budget during the glacial-interglacial transition. The similarity between the Taylor Dome $\delta^{13}\text{C}_{\text{ATM}}$ record and the previously reported measurements from the Byrd ice core [Leuenberger et al., 1992] supports the $\delta^{13}\text{C}_{\text{ATM}}$ ice core records, although the technical uncertainty in measuring $\delta^{13}\text{CO}_2$ remains significant (around 0.1‰).

[5] The interpretation of the glacial-interglacial transitions in $\delta^{13}\text{C}_{\text{ATM}}$ inferred from these ice cores poses a problem for the approach that assumes that the land carbon exerts control on $\delta^{13}\text{C}_{\text{ATM}}$. Estimations of changes in the terrestrial carbon cycle based on foraminifera $\delta^{13}\text{C}$ [Shackleton, 1977], the paleobiome distribution [Adams et al., 1990; Crowley, 1995; Maslin et al., 1995; Guiot et al., 2001], or the simulation of terrestrial biosphere models [Prentice et al., 1994; Francois et al., 1998; Beerling, 1999] reveal a decline in the carbon storage capacity of the land biosphere by $440\text{--}1350$ Pg C during the last glacial maximum (LGM) compared to the present day terrestrial carbon storage, with a best estimate of about 750 Pg C. Adding additional 750 Pg of terrestrial carbon to the atmosphere would have led to a change in $\delta^{13}\text{C}_{\text{ATM}}$ of about -0.4‰ (without accounting for changes in distribution of C_3/C_4 plants) which is significantly higher than the value of -0.16‰ inferred from the Taylor Dome ice core data [Smith et al., 1999]. Another potential source of carbon to the atmosphere during the LGM is associated with peat storage. The peat accumulation in the northern peatlands during the Holocene is estimated in $300\text{--}500$ Pg C [Laine et al., 1996; Gajewski et al., 2001]; presumably, during the glacial period this carbon was stored in the ocean. If one increases the changes in terrestrial carbon during the glacial-interglacial transition by additional $300\text{--}500$ Pg C, the discrepancy between the results by the approach based on land carbon control on $\delta^{13}\text{C}_{\text{ATM}}$ and the ice core data becomes even larger.

[6] Here we examine the contribution from the marine and the terrestrial biota to changes in the global carbon budget during the last glacial termination. The primary goal of our study is to investigate the possible influence of changes in the functioning of the marine biota during the

glacial-interglacial transition on the atmospheric CO₂ level and $\delta^{13}\text{C}_{\text{ATM}}$. For this purpose the climate system model CLIMBER-2 is used, which allows a fully interactive simulation of the glacial-interglacial changes in the physical and the chemical components of atmosphere, ocean, and biosphere.

[7] The paper is organized in the following way. First we analyze the role of the marine biota in the global carbon cycle by performing a set of sensitivity experiments under present day conditions. Then a similar set of sensitivity experiments are carried out under LGM conditions. Assuming a scenario with a stronger biological cycling of carbon in the ocean, the model reproduce the glacial atmospheric CO₂ level and $\delta^{13}\text{C}_{\text{ATM}}$ in accordance with the values inferred from the ice cores. Finally, we suggest that the abrupt changes in $\delta^{13}\text{C}_{\text{ATM}}$ inferred from the Taylor Dome ice core record are a consequence of changes in the marine biology.

2. Methods

[8] We performed a set of experiments with a climate system model of intermediate complexity CLIMBER-2 [Petoukhov *et al.*, 2000; Ganopolski *et al.*, 2001], version 2.3. It includes a 2.5-dimensional dynamical-statistical atmosphere model, a multibasin, zonally averaged ocean model (including a sea ice model) and a terrestrial vegetation model (including a model for the terrestrial carbon cycle) with a coarse spatial resolution of 10° in latitude and 51° in longitude. In version 2.3 of CLIMBER-2, the latitudinal resolution of oceanic model is increased to 2.5°. The time step differs among the model components (1 day, 5 days, and 1 year for atmospheric, ocean, and vegetation models, respectively). Results of CLIMBER-2 compare favorably with data of present-day climate and with paleoclimatic reconstructions [Ganopolski *et al.*, 1998; Claussen *et al.*, 1999]. The model is recently upgraded by the implementation of a marine carbon cycle model, which accounts for the cycling of inorganic and organic carbon in ocean [Brovkin *et al.*, 2002]. The marine biota model is similar to the model by Six and Maier-

Reimer [1996] and includes the distribution of phytoplankton, zooplankton, dissolved organic carbon (DOC), detritus (POC), phosphate, and the stable carbon isotopes.

[9] Regarding setup of the boundary conditions, the simulations are subdivided into three groups (see Table 1). The first group includes control simulations for present-day (PD) and LGM climates (LGM-Ctrl) with fixed atmospheric CO₂ concentration (280 and 200 ppmv for PD and LGM-Ctrl, respectively). Models for terrestrial and oceanic biogeochemistry simulate the global carbon cycle in equilibrium with prescribed atmospheric CO₂. Simulation PD serves as a reference simulation for biogeochemistry; it sets initial conditions for the total carbon storage in the system (ocean, land, and atmosphere) for the LGM scenarios with interactive carbon cycle. Let us note that in simulation LGM-Ctrl the total amount of carbon in the system differs from the carbon storage in the PD simulation and carbonate compensation is not considered. The purpose of the simulation LGM-Ctrl is to estimate the effects of changes in sea surface temperatures (SSTs) and oceanic circulation on the oceanic carbon storage.

[10] The second set of simulations of the oceanic carbon cycle without oceanic biology (frequently called as the “Strangelove ocean”) is aimed to estimate C_{OB} in the ocean for present-day (S-PD) and LGM climates (S-LGM). In the simulations, the physical climate state (temperature, precipitation, atmospheric, and oceanic circulation, etc.) is identical to the state from the control simulations. Similar to the LGM-Ctrl simulation, the total amount of carbon in the system is not conserved, and carbonate compensation is not accounted for. This limits the application of the Strangelove ocean simulations to the estimate of C_{OB} .

[11] The third group of simulations consists of several LGM scenarios (LGM, LGM-peat, and LGM-rr) that result in a draw down of the atmospheric CO₂ concentration from 280 to 200 ppmv. The purpose of these scenarios is to estimate changes in $\delta^{13}\text{C}_{\text{ATM}}$ in accordance with different

Table 1. Simulation Summary

Acronym	Simulation Purpose	Carbon Conservation	Atm. CO ₂ , ppmv	δ ¹³ C _{ATM} , ‰	Averaged ALK, μeq/kg	Averaged PO ₄ , μeq/kg	Export flux Np, Pg C/yr
<i>Control</i>							
PD	reference	–	280	–6.50	2373	2.08	7.2
LGM-Ctrl ^a	effect of SSTs and circulation changes on C _O	no ^b	200	–	2451	2.15	6.7
<i>Strangelove Ocean</i>							
S-PD	C _{OB} estimation	no ^b	280	–	2373	–	–
S-LGM ^a	C _{OB} estimation	no ^b	200	–	2576	–	–
<i>LGM Scenarios</i>							
LGM ^{a,c,d}	enhanced bio-pump	yes ^e	199	–6.56	2576	2.86	11.1
LGM-peat ^{a,d,f}	lower land carbon storage	yes ^g	198	–6.65	2621	2.86	11.6
LGM-r ^{a,c,h}	decreased rain ratio	yes ⁱ	200	–6.59	2607	2.57	10.0

^aBoundary conditions as for 21,000 yr before present: Insolation following Berger [1996], ice sheet distribution in accordance with Peltier [1994], salinity, alkalinity, and PO₄ concentration increased by 3.3% to account for sea level changes.

^bAtmospheric CO₂ concentration is constant; total carbon amount in the system is not conserved.

^cPhytoplankton growth rate is doubled under constraint of PO₄ limitation.

^dPO₄ concentration is higher than in LGM-Ctrl by 33%.

^eTotal carbon storage (land, atmosphere, and ocean) equals to a sum of the total carbon storage in the PD-simulation and dissolved CaCO₃ sediments (970 Pg C).

^fTransfer of terrestrial carbon is increased by 360 Pg C. Phytoplankton growth rate is increased 2.5 times under constraint of PO₄ limitation.

^gTotal carbon storage (land, atmosphere, and ocean) equals to a sum of the total carbon storage in the PD-simulation, dissolved CaCO₃ sediments (1330 Pg C), and peat carbon (360 Pg C).

^hRain ratio is decreased from 0.1 to 0.07. PO₄ concentration is higher than in LGM-Ctrl by 20%.

ⁱTotal carbon storage (land, atmosphere, and ocean) equals to a sum of the total carbon storage in the PD-simulation and dissolved CaCO₃ sediments (1220 Pg C).

hypothesis. The carbon cycle in these simulations is interactive; that is, the total amount of carbon stored in the ocean, land, and atmosphere is the same as in the PD-simulation. Because dissolution of the oceanic carbonate sediment plays an important role in the glacial biogeochemistry, a difference in the carbonate storage is included into the total carbon balance (see Table 2). The amount of dissolved carbonates is determined on a base of keeping the constant concentration of carbonate ion in the deep Pacific. Atmospheric and ocean models are interactive in the simulations; they respond to the atmospheric CO₂ as greenhouse gas forcing. If atmospheric CO₂ concentration in simulations were significantly different from the control level (200 ppmv), simulated climate state would be different from the control simulation (LGM-Ctrl), causing undesirable feedback loops to the carbon cycle. Therefore parameters of scenarios, for example, degree of enhancing of biological productivity in

the ocean, are chosen under condition that the atmospheric CO₂ concentration is ~ 200 ppmv. This approach guarantees that the climate state (e.g., temperature, precipitation, circulation) in the

Table 2. Global Carbon Balance in the Simulations PD and LGM

Compartment	Carbon, Pg	δ ¹³ C
<i>Preindustrial (PD)</i>		
Atmosphere (280 ppmv CO ₂)	600	–6.5
Land	1,920	–22.6
Ocean, DIC and DOC	38,330	0.4
Oceanic carbonate sediments	970	1.5
Total	41,820	
<i>Last Glacial Maximum (LGM)</i>		
Atmosphere (199 ppmv CO ₂)	420	–6.6
Land	1,280	–22.6
Ocean, DIC and DOC	40,120	0
Total	41,820	

LGM scenarios is the same as in the LGM-Ctrl simulation.

3. Results

3.1. Preindustrial Carbon Cycle

[12] The control simulation (PD) corresponds to preindustrial boundary conditions with an atmospheric CO_2 value of 280 ppmv and a $\delta^{13}\text{C}_{\text{ATM}}$ value of -6.5‰ (see Table 1). The model is integrated for 10,000 years achieving a steady state. The amount of carbon stored in the terrestrial pool is ~ 1920 Pg C (around 840 Pg C in the biomass and 1080 Pg C in the soil), with most of the carbon (around 85%) allocated to the C_3 -photosynthesis pathway and the remaining carbon (15%) to the C_4 -pathway. Owing to the fact that atmospheric CO_2 is depleted in ^{13}C by -6.5‰ , the average $\delta^{13}\text{C}$ of the terrestrial carbon cycle is about -22.6‰ (see Table 2). The ocean carbon storage consists of 38,250 and 80 Pg C in the form of DIC and DOC, respectively (the refractory DOC with thousand years timescale is not accounted for in the model). The marine primary productivity is ~ 44 Pg C yr^{-1} and the export flux N_p is ~ 7 Pg C yr^{-1} . These fluxes are comparable with the model estimates by *Six and Maier-Reimer* [1996]. The ^{13}C fractionation between DIC and marine phytoplankton is simulated as a function of dissolved molecular carbon dioxide [$\text{CO}_2(\text{aq})$] [*Rau et al.*, 1989; *Hofmann et al.*, 2000] which yields a globally averaged fractionation of -23‰ . Because the surface ocean $\delta^{13}\text{C}_{\text{DIC}}$ values are close to 2‰ in the model, the average $\delta^{13}\text{C}$ of the POC and DOC ($\delta^{13}\text{C}_{\text{POC}}$ and $\delta^{13}\text{C}_{\text{DOC}}$, respectively) is about -21‰ . The averaged $\delta^{13}\text{C}_{\text{DIC}}$ in the ocean equals 0.4‰ (see Table 2).

[13] To estimate the potential of the marine biological carbon pump in sequestering atmospheric CO_2 , we conducted the Strangelove ocean experiment (S-PD). The marine primary productivity was set to zero while the atmospheric CO_2 was kept at a constant value of 280 ppmv and $\delta^{13}\text{C}_{\text{ATM}}$ at value of -6.5‰ . After 10,000 years of integration the system approaches an equilibrium where the ocean has released around 2400 Pg C into the atmosphere and the averaged ocean $\delta^{13}\text{C}_{\text{DIC}}$ has increased to

2‰ . If the atmospheric CO_2 were interactive with the ocean, the corresponding increase of the atmospheric CO_2 level would be around 220 ppmv; this estimate is consistent with the increase of around 230 ppmv obtained in the Strangelove ocean experiment with a three-dimensional (3-D) oceanic carbon cycle model HAMOCC [*Maier-Reimer et al.*, 1996].

[14] To illustrate the results, a simplified view on the functioning of the global carbon cycle within the model is shown in Figure 1a. In the ocean, the total dissolved carbon, C_O , is separated into two pools: Abiotic carbon pool absorbed by the ocean due to the solubility pump, C_{OA} , and carbon cycled by the biological pump, C_{OB} , which consists of DOC of marine origin (river transport of terrestrial DOC is not accounted for in the model) as well as of DIC originated from remineralization of POC and DOC. The oceanic carbon storage in the S-PD-simulation is taken as an estimate of C_{OA} ; the rest of the total oceanic carbon in the PD-simulation is assumed to be an estimate for C_{OB} . In this simplification, the indirect influence of marine biota on the solubility pump through changes in the surface alkalinity is neglected. With this separation, the carbon pools with homogeneous ^{13}C fractionation can be considered separately; the average $\delta^{13}\text{C}_{\text{DIC}}$ from S-PD-simulation and $\delta^{13}\text{C}_{\text{DOC}}$ from PD-simulation are taken as estimates for $\delta^{13}\text{C}$ of C_{OA} and C_{OB} , respectively. The abiotic carbon cycle contains $\sim 35,900$ Pg C with a $\delta^{13}\text{C}$ value of 2‰ , and the biological cycle has a capacity of ~ 2400 Pg C and a $\delta^{13}\text{C}$ value of -21‰ . The total oceanic carbon content is $\sim 38,300$ Pg C, with an averaged $\delta^{13}\text{C}_{\text{DIC}}$ of $\sim 0\text{‰}$, both in line with GEOSECS inventory [*Bainbridge*, 1981; *Broecker et al.*, 1982; *Kroopnik*, 1985]. The terrestrial carbon storage is ~ 1900 Pg C and possesses an average $\delta^{13}\text{C}$ value of about -23‰ , in line with the other estimations for the preindustrial terrestrial carbon cycle [*Melillo et al.*, 1996].

[15] The two biological branches of the global carbon cycle, the terrestrial and the oceanic one, have very similar carbon isotopic signatures and carbon storage capacities. Therefore it is nearly impossible to separate their influence on the atmospheric isotope signature as well as the CO_2 con-

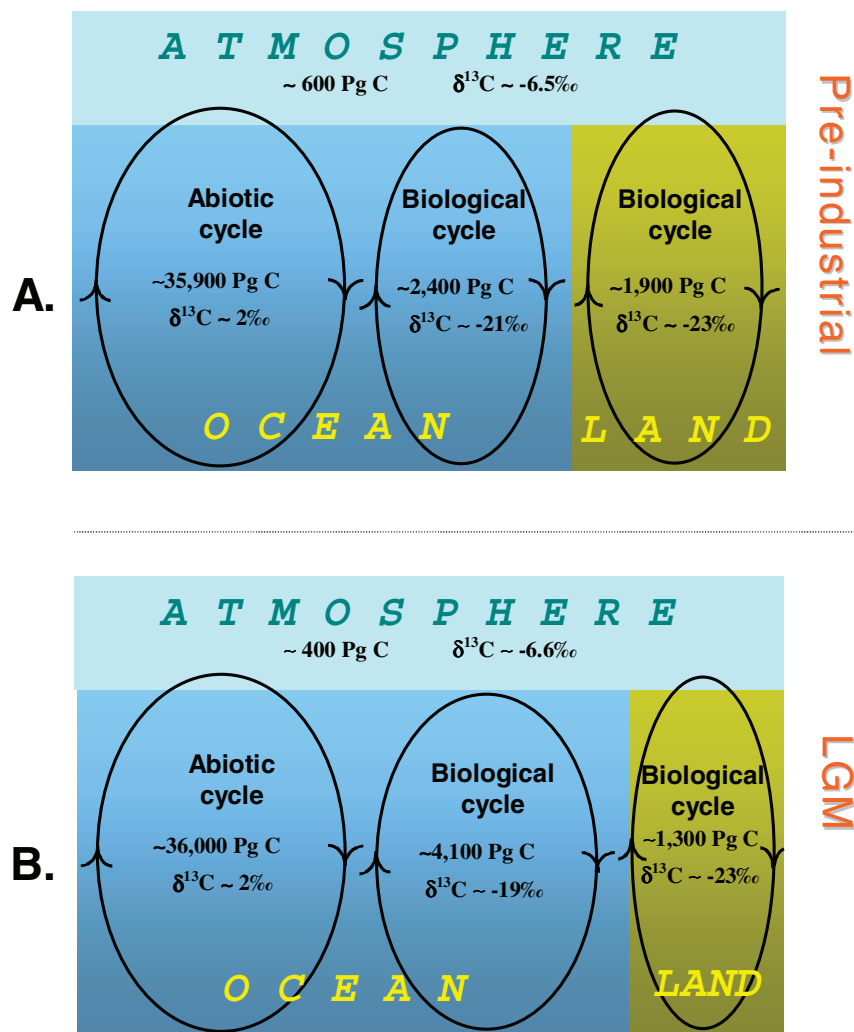


Figure 1. A simplified view of the global carbon cycle. (a) Simulation PD is shown. The oceanic carbon cycle is separated into an abiotic cycle (DIC absorbed by the solubility pump) and a biological cycle (DOC and DIC originated from remineralization of organic matter). Organic carbon of terrestrial and marine origin is isotopically much lighter ($\delta^{13}\text{C}$ of -21 to -23‰) than the DIC absorbed by the solubility pump ($\delta^{13}\text{C} \sim 2\text{‰}$). (b) Simulation LGM is shown. The terrestrial carbon storage is lower by 640 Pg C in comparison with the PD-simulation. This amount of isotopically light carbon enters the oceanic carbon cycle without substantial effect on the atmospheric $\delta^{13}\text{C}$ because of enhanced biological cycle in the ocean. The $\delta^{13}\text{C}$ of the oceanic biological cycle increases by 2‰ due to a drop in $[\text{CO}_2(\text{aq})]$.

centration using atmospheric data records alone. Any change in the atmospheric gas composition could be equally interpreted as changes in either the marine or the terrestrial biota branch of the global carbon cycle.

3.2. LGM Carbon Cycle

[16] In the experiments for the LGM, the model was driven by the orbital forcing corresponding to

the insolation 21,000 yr before present [Berger, 1996]. The ice sheet distribution and changes in the land area were taken from the PMIP reconstruction [Peltier, 1994]. Ocean volume and concentrations of oceanic tracers (salinity, alkalinity, nutrients) were adjusted to changes in the global sea level (see Table 1) in accordance with the SPECMAP reconstruction [Imbrie et al., 1984]. In the first simulation (LGM_Ctrl), the atmospheric CO_2 level was prescribed to a value of

200 ppm [Barnola *et al.*, 1987; Smith *et al.*, 1999] for the atmospheric model and the terrestrial biogeochemistry model while the atmospheric CO₂ used for calculating the air-sea exchange into the ocean model was kept at the pre-industrial level of 280 ppm. Corresponding changes in the oceanic circulation and atmospheric fields were described by Ganopolski *et al.* [1998] and Ganopolski and Rahmstorf [2001]. In comparison with PD-simulation, the global averaged annual mean air temperature and sea surface temperatures (SSTs) decrease by 5°C and 3°C, respectively, and the oceanic carbon storage is lower by 270 Pg C. Most of this decrease is explained by a decrease in the export flux, N_p , by 0.5 Pg C corresponding to around 8% of the preindustrial level. The draw down of the atmospheric CO₂ concentration caused by the increased solubility of the relatively cold surface waters [see, e.g., Broecker and Peng, 1982; Hofmann *et al.*, 1999; Archer *et al.*, 2000b; Schulz *et al.*, 2001] is not significant in our simulation. The model sensitivity of the oceanic carbon uptake on changes in the SSTs is critical dependent upon the parameterization of vertical and horizontal mixing [Archer *et al.*, 2000a]. In accordance with other ocean circulation models with a relatively large mixing, the carbon uptake in the CLIMBER model is not significantly influenced by changes in the SSTs during the LGM-simulations. The sea surface temperatures, in the polar convection regions where the deep water is formed, are not considerably changed because the temperature here is locked to the freezing temperature of sea water. The impact of Antarctic sea-ice changes on the atmospheric CO₂ concentration [Stephens and Keeling, 2000; Maqueda and Rahmstorf, 2002] is negligible in the CLIMBER model similar to the HAMOCC model (D. Archer *et al.*, Effect of Antarctic sea ice and stratification on atmospheric $p\text{CO}_2$: A box model artifact?, manuscript submitted to *Paleoceanography*, 2001). Moreover, the ocean should absorb additional 640 Pg C released from the terrestrial biosphere because the terrestrial carbon storage capacity is drastically reduced due to the decrease in the forest area as well as in the plant primary productivity.

[17] Currently, most of the hypothesis proposed to explain glacial-interglacial transitions in the global carbon cycle can be subdivided into two types: changes in (1) the marine solubility pump (carbonate or silicate oceanic chemistry) or in (2) the marine biological pump (biological productivity) (for review, see Archer *et al.* [2000a, 2000b] and Sigman and Boyle [2000]). Iron fertilization experiments recently conducted in the Southern Ocean (SO) (SOIREE [Boyd *et al.*, 2000], EisenEx [Smetacek, 2001]), spot this region as a mainly iron limited area with respect to primary production of phytoplankton. Hence the iron fertilization hypothesis by Martin [1990], which explains the lower atmospheric CO₂ levels during LGM by a stimulated growth of phytoplankton owing to a much higher aeolian dust supply to the SO (hypothesis 2), becomes again favored in the understanding of glacial-interglacial transitions. The assumption of a strengthened biological productivity during glacial periods is also in line with SO₄ proxies [Mayewski *et al.*, 1996; Broecker and Henderson, 1998] while in disagreement with some other proxies, for example, Cd/P ratio [Elderfield and Rickaby, 2000].

[18] To achieve an atmospheric CO₂ level drop of 80 ppmv, we carried out a simulation (LGM) with a mixture of the two hypotheses 1 and 2 discussed above (Table 1). The global mean nutrient concentration in the ocean was increased by 33% imitating nutrients washout from the continents [see, e.g., Shaffer, 1990]. Additionally, a growth rate of phytoplankton was increased globally by a factor of 2 simulating an enhancement of the biological pump due to iron fertilization [Hofmann *et al.*, 1999; Watson *et al.*, 2000]. This results in a 55% increase in the export flux. The increased flux of organic matter to the interior of the ocean and the subsequent remineralization results in lower oxygen levels during the LGM than in the present ocean (see Figure 2). In particular, oxygen level in the intermediate waters in the equatorial Pacific becomes very low, owing to the high export flux and the relatively low oxygen concentration in the deep waters there. The lysocline constraint imposed by sediment cores [Sigman *et al.*, 1998] is considered by keeping a constant carbonate ion concen-

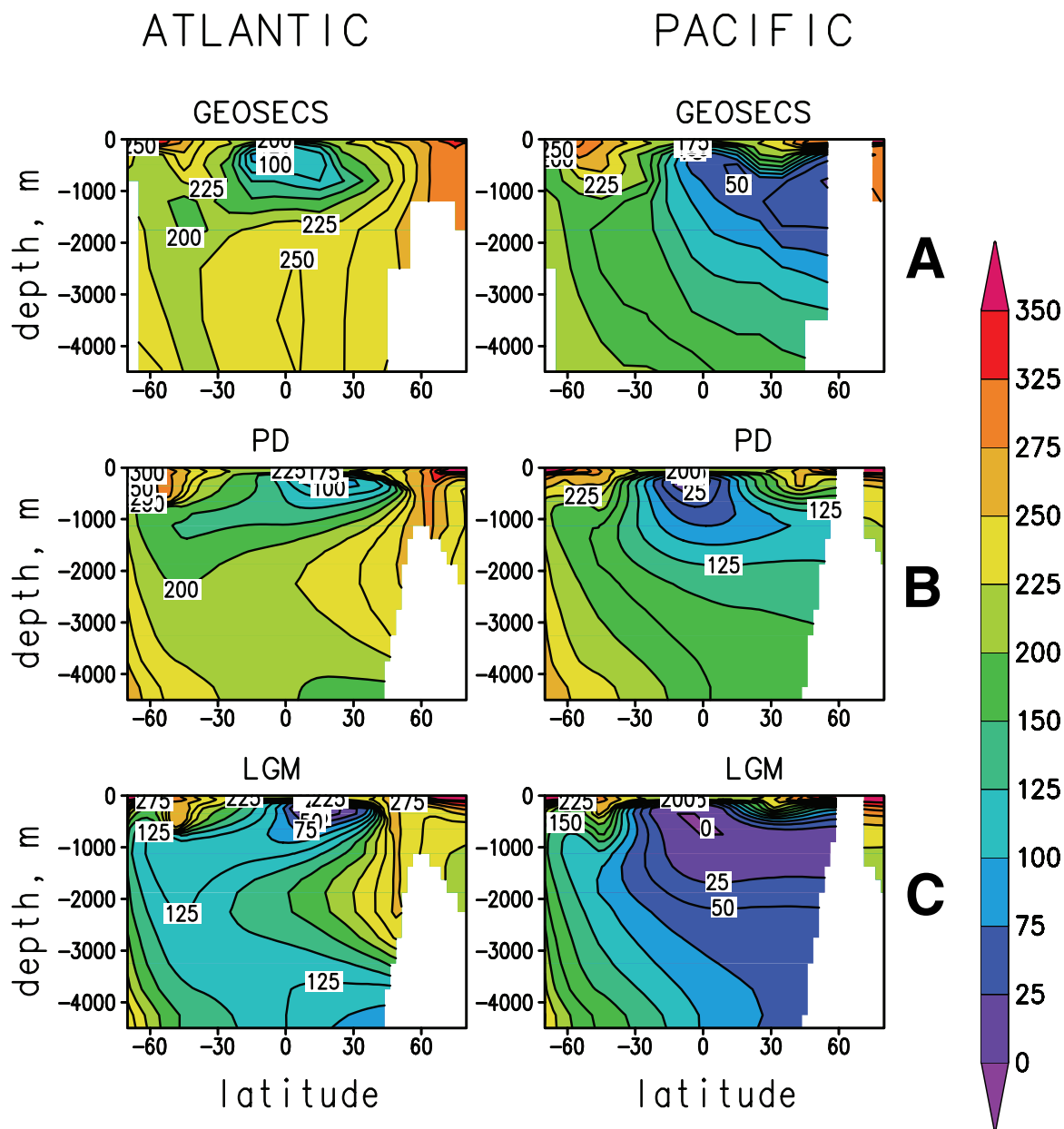


Figure 2. Oxygen concentration, $\mu\text{mol/kg}$. (a) Observations GEOSECS. (b) Simulation PD. (c) Simulation LGM.

tration in the deep Pacific. Additional dissolution of calcium carbonate from the sediments is modelled by adding 970 Pg carbon to the system and correspondingly increase the oceanic alkalinity in a proportion of 2 equivalent per 1 mole of carbon. This simplified approach neglect, to a first approximation, the influence of increased downward flux of organic matter and carbonate shells on the complex remineralization processes in the sediments which influence the pH of the deep ocean

and the process of carbonate dissolution [Archer, 1991].

[19] In response to the stronger biological and solubility carbon pumps, the oceanic DIC pool increases by around 1800 Pg C (Table 2). Because most of this increase is due to an enhanced biological pump, the average oceanic $\delta^{13}\text{C}_{\text{DIC}}$ drops considerably. However, $\delta^{13}\text{C}_{\text{POC}}$ increases by 2‰ because of the drop in $[\text{CO}_2(\text{aq})]$. Surface ocean

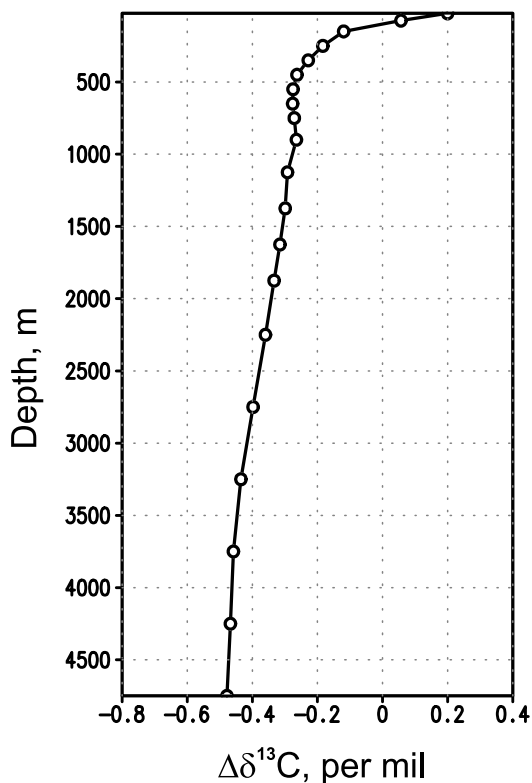


Figure 3. Depth profile of globally averaged changes in $\delta^{13}\text{C}_{\text{DIC}}$, difference between simulations LGM and PD.

$\delta^{13}\text{C}_{\text{DIC}}$ is higher by 0.2‰ because of the enhanced biological production. The gradient in $\delta^{13}\text{C}_{\text{DIC}}$ between the surface and the deep ocean increases by 0.7‰ (see Figure 3). The fractionation of terrestrial carbon decreases by 0.1‰ because of a relative advance of C_4 plants [Francois *et al.*, 1999; Beerling, 1999]. Finally, atmospheric CO_2 is 199 ppmv and $\delta^{13}\text{C}_{\text{ATM}}$ is -6.56‰ . The latter value is only by 0.06‰ lower than in simulation (PD). To explore an effect of changes in marine biota on the carbon cycle, a simulation (S-LGM) without a marine biota similar to simulation (S-PD) is carried out. Oceanic carbon storage in the simulation (S-LGM) is 36,000 Pg C, and a difference in oceanic carbon between simulations (LGM) and (S-LGM) is 4,100 Pg C (see Figure 1b). We conclude that most of the increase in the oceanic carbon storage, or 1700 Pg C, is due to the enhanced biological pump in the ocean, and that the increase in the oceanic carbon storage due to solubility pump is only 100 Pg C. In other words, the biological

carbon cycle within the model should be enhanced by $\sim 70\%$ for glacial conditions in order to obtain glacial-interglacial changes in CO_2 similar to the ones inferred from the ice cores.

[20] The terrestrial biogeochemistry model in CLIMBER-2 does not simulate the accumulation of carbon in peatlands. The current estimates of peat carbon accumulated in the northern peatlands during the Holocene range from 300 to 500 Pg C [Laine *et al.*, 1996]. Accounting for the glacial-interglacial changes in the peat carbon leads to an additional transfer of terrestrial carbon into the ocean during the LGM. Addressing the uncertainties in the terrestrial carbon budget, a simulation (LGM-peat) was carried out where additional 360 Pg C of terrestrial carbon with $\delta^{13}\text{C}$ of -22.6‰ (averaged $\delta^{13}\text{C}$ of terrestrial carbon in simulation PD) were added to the model. The total transfer of terrestrial carbon from the land into the ocean is then 1000 Pg C. The growth rate for oceanic phytoplankton was additionally increased (2.5 times in comparison with the PD-simulation) which corresponds to a hypothesis of stronger enhancement of the biological pump than in the LGM-simulation. As result, the biological productivity increased additionally by 0.7 Pg C and the biological carbon storage, C_{OB} , increased by around 170 Pg C. Additional 360 Pg C of carbonate sediments were dissolved to account for the carbonate compensation in the ocean. In response to these forcings, the mean ocean alkalinity increased by 45 $\mu\text{mol/kg}$ (see Table 1) and the carbonate ion concentration in the deep ocean was not significantly changed. Equilibrium atmospheric CO_2 in this simulation is 198 ppmv and $\delta^{13}\text{C}_{\text{ATM}}$ is -6.65‰ , similar to the value of $\delta^{13}\text{C}_{\text{ATM}}$ for the LGM inferred from the Taylor Dome data (-6.67‰ , see section 4 below). Adding 360 Pg C of organic carbon into the system resulted in a decrease of $\delta^{13}\text{C}_{\text{ATM}}$ by 0.09‰, similar to a decrease by 0.1‰ expected from the simplified calculations (see the third paragraph in appendix A).

[21] In the simulations (LGM) and LGM-peat, the rain ratio (ratio of carbonate flux to the export flux) is the same as in the PD-simulation. Assuming the

same rain ratio, a strengthening of the biological pump in the LGM scenarios would also enhance formation of calcareous shells by marine biota. Hence the burial rate of CaCO_3 into the sediments would increase similarly, shifting the deep ocean to more acid conditions. This would counteract the initial atmospheric CO_2 draw down, even were the CO_3^{2-} concentration in the deep ocean to be kept constant. To address this potential shortcoming of the scenarios, another simulation (LGM-rr) was done with enhanced biological pump but with the rain ratio decreased to such a level that CaCO_3 flux is the same as in the PD-simulation. A rationale for the latter assumption is a possible shift in glacial marine ecosystems toward dominance of silica-limited phytoplankton (diatoms) over nonsiliceous species including coccoliths, which have calcareous shells: increased dust deposition rates during glacial times presumably provided the oceans with a higher silica input, releasing diatoms from SiOH_4 stress [Harrison, 2000; Treguer and Pondaven, 2000]. Decrease in the rain ratio leads to a more efficient biological pump, which does not need to be as strongly enhanced as in the LGM-simulation. In the LGM-rr-simulation, a control level of the atmospheric CO_2 concentration (200 ppmv) was achieved by increasing of the PO_4 inventory by 20% and by doubling of the phytoplankton growth rate. The export flux is 10 Pg C/yr and the amount of dissolved carbonate is 1220 Pg C. Decrease in the oceanic biological pump results in smaller $\delta^{13}\text{C}_{\text{ATM}}$ (-6.59‰) than in the LGM-simulation. The decrease in $\delta^{13}\text{C}_{\text{ATM}}$ in response to decrease in biological productivity is in line with simulations by Marino *et al.* [1992] who attributed decrease in $\delta^{13}\text{C}_{\text{ATM}}$ during glacial period to reduction in terrestrial biomass and decreased oceanic productivity.

4. Discussion: Interpretation of the Ice Core Data

[22] Recently, Smith *et al.* [1999] presented an atmospheric record inferred from the Taylor Dome ice core, covering the time period from 26 kyr BP until 2 kyr BP. The original data, as depicted in Figure 4 (filled circles with a 1σ error bar), were interpolated within a time interval of 1000 years (solid line). The end of the LGM is taken to be at

17.5 kyr BP following Smith *et al.* [1999], and the onset of the Holocene is chosen at 11.2 kyr BP in accordance with Monnin *et al.* [2001]. For the time period between 26 and 17.5 kyr BP, which includes the LGM, the mean atmospheric CO_2 level is of ~ 192 ppmv and the $\delta^{13}\text{C}$ value of about -6.65‰ . During the Holocene (11.2 to 2 kyr BP) the mean atmospheric CO_2 level as well as the $\delta^{13}\text{C}_{\text{ATM}}$ value has increased with respect to the LGM (26–17.5 kyr BP) by 79 ppmv and 0.17‰, respectively. This is in agreement with the observations by Leuenberger *et al.* [1992], who found a ΔCO_2 shift of 80 ppmv and a shift in $\delta^{13}\text{C}_{\text{ATM}}$ of 0.19‰ between LGM and Holocene in the Antarctic ice core.

[23] The averaged shift in $\delta^{13}\text{C}_{\text{ATM}}$ of around 0.17‰ inferred from the Taylor Dome ice core is significantly smaller than the value one could expect assuming that the terrestrial biosphere controls $\delta^{13}\text{C}_{\text{ATM}}$ values alone. Smith *et al.* [1999] argued that, due to an SST lowering by 5°C during LGM, the stable carbon isotope fractionation of the air-sea gas-exchange was enhanced by around 0.6‰ [Mook, 1987]. This could explain the higher value of oceanic $\delta^{13}\text{C}_{\text{DIC}}$ and the corresponding low value of atmospheric $\delta^{13}\text{C}$ at 16.5 kyr BP. However, our simulation does not support this hypothesis because of two reasons. First the global averaged SST is lower in the simulation (LGM) by 3°C , while the SSTs in the areas of deep water formation is not considerably changed. Second, the ^{13}C fractionation associated with the air-sea gas exchange depends linearly on the fraction of the bicarbonate ion [Siegenthaler and Münnich, 1981; Zhang *et al.*, 1995], which is lower by 4% in the LGM simulation because of the lower CO_2 and higher alkalinity (see the second paragraph in appendix A). As a result, changes in the fractionation in the solubility pump cannot explain the observed shift in $\delta^{13}\text{C}_{\text{ATM}}$ within the model.

[24] Considering the sensitivity study above, we suggest the following scenario for the last glacial-interglacial transition: During the LGM the oceanic biological and solubility pumps worked in an enhanced mode, compared with the Holocene conditions. At the beginning of the deglaciation, around 17.5 kyr BP, a decrease in the aeolian iron supply into the SO [Petit *et al.*, 1990] led to a

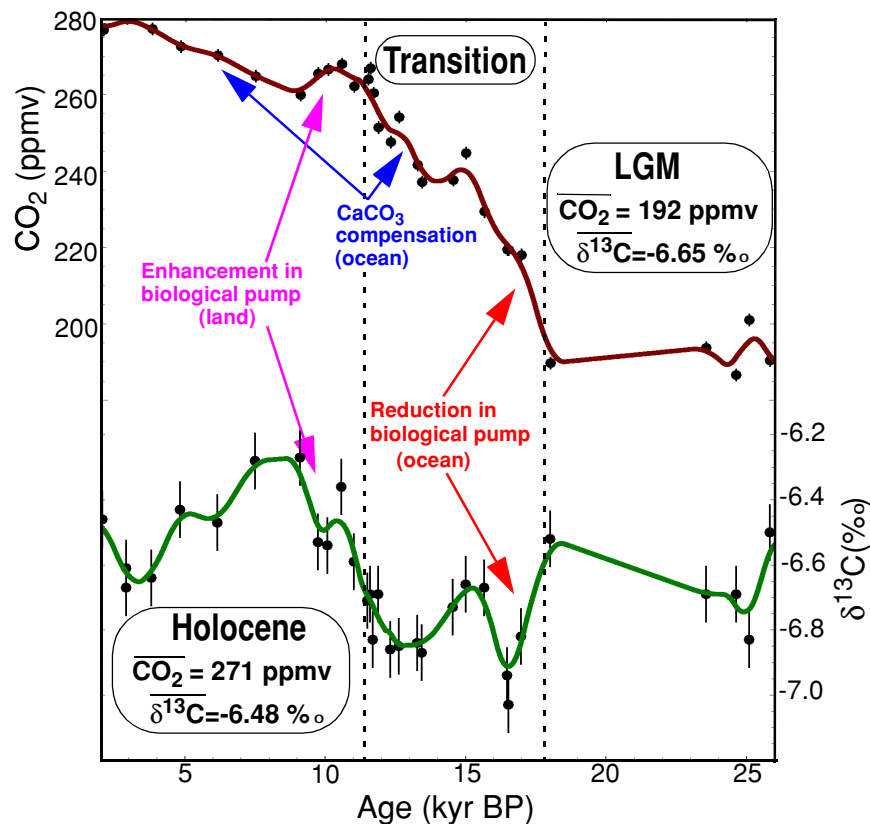


Figure 4. Interpretation of the Taylor Dome ice core data [Smith *et al.*, 1999]. The original data for 26–2 kyr BP are shown by filled circles with a 1σ error bar. The upper and lower curves are 1000 year moving average for atmospheric CO_2 concentration and $\delta^{13}\text{C}_{\text{ATM}}$, respectively. Vertical dashed lines indicate boundaries between the LGM, transition, and the Holocene. Averaged atmospheric CO_2 and $\delta^{13}\text{C}_{\text{ATM}}$ for LGM and Holocene are shown in the rounded boxes. Red arrows point to the simultaneous increase in the atmospheric CO_2 and decrease in $\delta^{13}\text{C}_{\text{ATM}}$ at the beginning of the transition, interpreted as a reduction in the oceanic biological pump. Blue arrows are for increase in the atmospheric CO_2 at the end of the transition and during the middle to late Holocene, presumably due to the carbonate compensation mechanism. Magenta arrows point on simultaneous slowdown of the atmospheric CO_2 growth and increase in $\delta^{13}\text{C}_{\text{ATM}}$ at the early Holocene, interpreted as an increase in the terrestrial carbon storage.

reduction of the strength of the ocean biological pump. A simultaneous decrease in the oceanic overturning due to an increased freshwater flux from the melting ice sheets could enhance this oceanic carbon release. The subsequent outgassing of CO_2 depleted in ^{13}C was followed by a simultaneous increase in CO_2 and a decrease in $\delta^{13}\text{C}_{\text{ATM}}$ (shown as red arrows in Figure 4). Decreases in the terrestrial carbon storage due to shrinking tropical land areas could potentially be an additional source of atmospheric carbon. However, the amplitude of the latter source cannot be considerable because of rather slow changes in sea level. Moreover, the general trend in the glacial-interglacial transition is

a reestablishment of forest and soil cover and thereby a corresponding uptake of carbon (640 Pg C within the model, see Table 2).

[25] We hypothesize that the oceanic biological pump reached an interglacial level ~ 13 – 14 kyr BP when the dust supply to the SO was significantly diminished. The impact of CaCO_3 compensation on atmospheric CO_2 starts several thousands of years after beginning of transition and results in higher accumulation rates of CaCO_3 (blue arrows in Figure 4). Additionally, the sea level rise started to contribute to enhanced carbonate and nutrient sedimentation in the continental shelf areas (blue

arrows in Figure 4). With the onset of the Holocene about 11 kyr BP, the terrestrial biosphere began to accumulate carbon depleted in ^{13}C , which resulted in a constant or declined level in atmospheric CO_2 and increased $\delta^{13}\text{C}_{\text{ATM}}$ values (shown as magenta arrows in Figure 4). Later during the Holocene, carbon storage in the terrestrial biosphere was not changed significantly [Beerling, 1999; Brovkin *et al.*, 2002]. A further increase of atmospheric CO_2 of ~ 20 ppmv from 8 to 2 kyr BP could be explained by the carbonate compensation due to excessive accumulation of carbonate sediments in the course of the Holocene [Milliman, 1993; Broecker *et al.*, 1999].

5. Conclusions

[26] We have simulated the glacial-interglacial difference in the global carbon budget with a fully interactive model of the climate system, which provides consistent changes in the atmospheric, oceanic, and terrestrial biogeochemistry. With a combination of an enhanced biological production and dissolution of CaCO_3 , the model simulates changes for glacial atmospheric CO_2 and $\delta^{13}\text{C}_{\text{ATM}}$ similar to those inferred from the ice cores.

[27] On the basis of these results, we suggest correcting the approach, which assumes that the land carbon exerts control on the atmospheric $\delta^{13}\text{C}$. The marine biology affects $\delta^{13}\text{C}_{\text{ATM}}$ value as well. Because both terrestrial and oceanic branches of the biological carbon cycle have very similar carbon isotopic signatures and carbon storage capacities, it is nearly impossible to separate their influence on the atmospheric isotope signature as well as the CO_2 level using atmospheric data records alone.

[28] An elevation of the $\delta^{13}\text{C}_{\text{ATM}}$ can also be caused by an increased storage of carbon in the terrestrial ecosystem. When changes in the terrestrial carbon pool are compensated by changes of the biological carbon pump in the ocean, the transfer of organic matter from land into the ocean and vice versa cannot be inferred from the records of the stable carbon isotope composition of the atmosphere. An increase of the terrestrial carbon pool would increase the $\delta^{13}\text{C}_{\text{ATM}}$, while the simultane-

ous weakening of the marine biological carbon pump would drive the $\delta^{13}\text{C}_{\text{ATM}}$ values in the opposite direction.

[29] The evidence from the ice core data supports this result. Particularly, a drop of 0.5‰ in $\delta^{13}\text{C}_{\text{ATM}}$ at the beginning of the transition period (around 16.5 kyr BP) combined with a simultaneous increase in the atmospheric CO_2 [Smith *et al.*, 1999] is very difficult to explain without including the marine biology. We interpret this drop as a substantial reduction in the oceanic biological pump, for example, as a consequence of a decrease in the biological production in the Southern ocean.

Appendix A. Sensitivity of $\delta^{13}\text{C}_{\text{ATM}}$ to Changes Terrestrial and Marine Biology

A.1. Conventional Approach: $\delta^{13}\text{C}_{\text{ATM}}$ is Controlled by Land Carbon Storage

[30] The global carbon budget is constrained by conservation equations for total carbon in the system, A , and total ^{13}C , A_{13} , expressed in $\delta^{13}\text{C}$ terms:

$$\sum C_i = A, \quad (\text{A1})$$

$$\sum C_i \delta_i = A_{13}, \quad (\text{A2})$$

where C_i and δ_i are for carbon and $\delta^{13}\text{C}$ of i th compartment for the preindustrial state, index $i = \{A, O, L\}$ is for atmosphere, ocean, and land, respectively. If ΔC_i and $\Delta \delta_i$ are changes in carbon and $\delta^{13}\text{C}$ between the glacial and the reference states, then equations (A1)–(A2) can be written in a form

$$\sum \Delta C_i = 0, \quad (\text{A3})$$

$$\sum \Delta \delta_i (C_i + \Delta C_i) + \sum \delta_i \Delta C_i = 0. \quad (\text{A4})$$

Let us assume that there are no changes in the isotopic fractionation on the atmosphere-ocean and atmosphere-land boundaries, as well as in the oceanic biology. In this case an equilibrium approximation could be applied:

$$\Delta \delta_A = \Delta \delta_O = \Delta \delta_L, \quad (\text{A5})$$

and from equation (A4) follows

$$\Delta\delta_A \sum C_i = - \sum \delta_i \Delta C_i. \quad (\text{A6})$$

From equations (A3) and (A6) one can estimate sensitivity of $\delta^{13}\text{C}_{\text{ATM}}$ to changes in terrestrial carbon storage ΔC_L . With preindustrial values of δ_i and C_i in the compartments taken from the Table 2 for (PD) simulation, ΔC_A taken from the observations and $\Delta C_O = -\Delta C_L$, 640 Pg C decrease in the terrestrial carbon storage corresponds to 0.36‰ decline in δ_A (ignoring changes in carbonate sediments). In this approach, atmospheric $\delta^{13}\text{C}$ is fully controlled by the changes in the terrestrial carbon storage. Sensitivity of $\delta^{13}\text{C}_{\text{ATM}}$ to changes in land carbon, $\Delta\delta_A/\Delta C_L$, is 0.1‰ per 180 Pg C. In other words, if additional 180 Pg C of terrestrial carbon are dissolved in the ocean, the atmospheric $\delta^{13}\text{C}$ is decreased by 0.1‰. Accounting for additional carbonate dissolution due to carbonate compensation leads to negligible changes in the sensitivity.

A.2. Correction for Inorganic Fractionation

[31] Equation (A5) is valid in case of constant oceanic fractionation factor, α_o . It is relatively easy to correct equation (A5) for the changes in inorganic fractionation by assuming

$$\Delta\delta_O = \Delta\delta_A + \Delta\delta_{of}, \quad (\text{A7})$$

where $\Delta\delta_{of}$ is a change in α_o due to changes in temperature and carbonate ion composition. The α_o increases by 0.1‰ with decrease in water temperature per °C [Mook *et al.*, 1974]. The factor α_o depends also on a fraction of bicarbonate ion $[\text{HCO}_3^-]$ in DIC species, with decrease $\sim 0.1\%$ per 1% decrease in $[\text{HCO}_3^-]$ fraction. If surface alkalinity increases, like in LGM-simulation, then $[\text{HCO}_3^-]$ fraction decreases, leading to a decrease in α_o . In LGM simulation, globally averaged SST decreases by 3°C, and the fraction of $[\text{HCO}_3^-]$ decreases by 4%. Consequently, $\Delta\delta_{of}$ is about -0.1% . Let us note that the correction for inorganic fractionation does not change the sensitivity of $\delta^{13}\text{C}_{\text{ATM}}$ to the changes in terrestrial carbon cycle.

A.3. Accounting for Changes in Marine Biology

[32] If marine biology is altered, equation (A5) is no longer valid. In this case, the ocean carbon cycle is affected by changes in biological export flux, N_p , and fractionation during marine photosynthesis, α_{MB} (see Figure 1). The effect of terrestrial carbon emission on $\delta^{13}\text{C}_{\text{ATM}}$ depends on whether this carbon is allocated into abiotic or biological cycle. In a scenario of additional carbon emission, for example, by peat mineralization like in the simulation (LGM-peat), the model can simulate its absorption by ocean by taking approximately 50% into biological cycle and 50% into abiotic cycle due to necessity to fulfil the lysocline constraint. This would lead to halving sensitivity of $\delta^{13}\text{C}_{\text{ATM}}$ to changes in land carbon, $\Delta\delta_A/\Delta C_L$, to 0.1‰ per 360 Pg C.

Acknowledgments

[33] The authors thank Martin Claussen, Miguel Maqueda, Stefan Rahmstorf, Colin Prentice, and an anonymous reviewer for the thoughtful comments. We appreciate help by David Archer whose suggestions and remarks lead to considerable improvement of the manuscript. Jørgen Bendtsen was funded by the Danish National Science Research Council.

References

- Adams, J. M., H. Faure, L. Faure-Denard, J. M. McGlade, and F. I. Woodward, Increases in terrestrial carbon storage from the Last Glacial Maximum to the present, *Nature*, 348, 711–714, 1990.
- Archer, D., Modeling the calcite lysocline, *J. Geophys. Res.*, 96, 17,037–17,050, 1991.
- Archer, D. E., G. Eshel, A. Winguth, W. Broecker, R. Pierrehumbert, M. Tobis, and R. Jacob, Atmospheric $p\text{CO}_2$ sensitivity to the biological pump in the ocean, *Global Biogeochem. Cycles*, 14, 1219–1230, 2000a.
- Archer, D., A. Winguth, D. Lea, and N. Mahowald, What caused the glacial/interglacial atmospheric CO_2 cycles?, *Rev. Geophys.*, 38, 159–189, 2000b.
- Bainbridge, A. E., *GEOSECS Atlantic Expedition*, vol. 1, *Hydrographic Data 1972–1973*, 121 pp., Natl. Sci. Foundation, Washington, D.C., 1981.
- Barnola, J. M., D. Raynaud, Y. S. Korotkevich, and C. Lorius, Vostok ice core provides 160,000-year record of atmospheric CO_2 , *Nature*, 329, 408–414, 1987.
- Battle, M., M. L. Bender, P. P. Tans, J. W. C. White, J. T. Ellis, T. Conway, and R. J. Francey, Global carbon sinks and their variability inferred from atmospheric O_2 and $\delta^{13}\text{C}$, *Science*, 287, 2467–2470, 2000.

- Beerling, D. J., New estimates of carbon transfer to terrestrial ecosystems between the last glacial maximum and the Holocene, *Terra Nova*, 11, 162–167, 1999.
- Berger, A., Orbital variations, in *Encyclopaedia of Climate and Weather*, edited by S. Schneider, pp. 557–564, Oxford Univ. Press, New York, 1996.
- Bird, M. I., J. Lloyd, and G. D. Farquhar, Terrestrial carbon-storage from the last glacial maximum to the present, *Chemosphere*, 33, 1675–1685, 1996.
- Boyd, P. W., et al., A mesoscale phytoplankton bloom in the polar Southern Ocean stimulated by iron fertilization, *Nature*, 407, 695–702, 2000.
- Broecker, W. S., and G. M. Henderson, The sequence of events surrounding Termination II and their implications for the cause of glacial-interglacial CO₂ changes, *Paleoceanography*, 13, 352–364, 1998.
- Broecker, W. S., and T. H. Peng, *Tracers in the Sea*, Lamont-Doherty Geological Observatory of Columbia University, Palisades, New York, 1982.
- Broecker, W. S., D. W. Spenger, and H. Craig, *GEOSECS Pacific Expedition*, vol. 3, *Hydrographic data 1973–1974*, 173 pp., Natl. Sci. Foundation, Washington, D.C., 1982.
- Broecker, W. S., E. Clark, D. C. McCorkle, T.-H. Peng, I. Hajdas, and G. Bonani, Evidence for a reduction in the carbonate ion content of the deep sea during the course of the Holocene, *Paleoceanography*, 14, 744–752, 1999.
- Brovkin, V., et al., Carbon cycle, vegetation, and climate dynamics in the Holocene: Experiments with the CLIMBER-2 model, *Global Biogeochem. Cycles*, in press, 2002.
- Ciais, P., P. P. Tans, M. Trolier, J. W. C. White, and R. J. Francey, A large northern hemisphere terrestrial CO₂ sink indicated by the ¹³C/¹²C ratio of atmospheric CO₂, *Science*, 269, 1098–1102, 1995.
- Claussen, M., A. Ganopolski, C. Kubatzki, V. Petoukhov, and S. Rahmstorf, A new model for climate system analysis: Outline of the model and application to paleoclimate simulations, *Environ. Modell. Assess.*, 4, 209–216, 1999.
- Crowley, T. J., Ice age terrestrial carbon changes revisited, *Global Biogeochem. Cycles*, 9, 377–389, 1995.
- Elderfield, H., and R. E. M. Rickaby, Oceanic Cd/P ratio and nutrient utilization in the glacial Southern Ocean, *Nature*, 405, 305–310, 2000.
- Francois, L. M., Y. Godderis, P. Warnant, G. Ramstein, N. de Noblet, and S. Lorenz, Carbon stocks and isotopic budgets of the terrestrial biosphere at mid-Holocene and last glacial maximum times, *Chem. Geol.*, 159, 163–189, 1999.
- Gajewski, K., A. Viau, M. Sawada, D. Atkinson, and S. Wilson, Sphagnum peatland distribution in North America and Eurasia during the past 21,000 years, *Global Biogeochem. Cycles*, 15, 297–310, 2001.
- Ganopolski, A., and S. Rahmstorf, Simulation of rapid glacial climate changes in a coupled climate model, *Nature*, 409, 153–158, 2001.
- Ganopolski, A., S. Rahmstorf, V. Petoukhov, and M. Claussen, Simulation of modern and glacial climates with a coupled global climate model, *Nature*, 391, 350–356, 1998.
- Ganopolski, A., V. Petoukhov, S. Rahmstorf, M. Claussen, A. Eliseev, and C. Kubatzki, CLIMBER-2: A climate system model of intermediate complexity. Part II: Validation and sensitivity tests, *Clim. Dyn.*, 17, 735–751, 2001.
- Goericke, R., and B. Fry, Variations of marine plankton δ¹³C with latitude, temperature, and dissolved CO₂ in the world ocean, *Global Biogeochem. Cycles*, 8, 85–90, 1994.
- Guiot, J., I. C. Prentice, C. Peng, D. Jolly, F. Laarif, and B. Smith, Reconstructing and modelling past changes in terrestrial primary production, in *Terrestrial Global Productivity*, edited by J. Roy, H. A. Mooney, and B. Saugier, pp. 479–498, Academic, San Diego, Calif., 2001.
- Harrison, K. G., Role of increased marine silica input on paleo-pCO₂ levels, *Paleoceanography*, 15, 292–298, 2000.
- Hofmann, M., W. S. Broecker, and J. Lynch-Stieglitz, Influence of a [CO₂(aq)] dependent biological C-isotope fractionation on glacial ¹³C/¹²C ratios in the ocean, *Global Biogeochem. Cycles*, 13, 873–883, 1999.
- Hofmann, M., D. A. Wolf-Gladrow, T. Takahashi, S. C. Sutherland, K. D. Six, and E. Maier-Reimer, Stable isotope composition of particulate organic matter in the ocean: A model study, *Mar. Chem.*, 72, 131–150, 2000.
- Imbrie, J., N. J. Shackleton, N. G. Pisias, J. J. Morley, W. L. Prell, D. G. Martinson, J. D. Hays, A. McIntyre, and A. C. Mix, The orbital theory of Pleistocene climate: support from a revised chronology of the marine δ¹⁸O record, in *Milankovitch and Climate: Understanding the Response to Astronomical Forcing, Part I*, edited by A. Berger et al., pp. 269–305, D. Reidel Publ., Norwell, Mass., 1984.
- Joos, F., and M. Bruno, Long-term variability of the terrestrial and oceanic carbon sinks and the budgets of the carbon isotopes ¹³C and ¹⁴C, *Global Biogeochem. Cycles*, 12, 277–295, 1998.
- Kroopnik, P. M., The distribution of ¹³C of ΣCO₂ in the world oceans, *Deep Sea Res.*, 32, 57–84, 1985.
- Laine, J., J. Silvola, K. Tolonen, J. Alm, H. Nykanen, H. Vasander, T. Sallantausta, I. Savolainen, J. Sinisalo, and P. J. Martikainen, Effect of water-level drawdown on global climatic warming: Northern peatlands, *Ambio*, 25, 179–184, 1996.
- Leuenberger, M., U. Siegenthaler, and C. C. Langway, Carbon isotope composition of atmospheric CO₂ during the last ice age from an Antarctic ice core, *Nature*, 357, 488–490, 1992.
- Lloyd, J., and G. D. Farquhar, ¹³C discrimination during CO₂ assimilation by the terrestrial biosphere, *Oecologia*, 99, 201–215, 1994.
- Maier-Reimer, E., U. Mikolajewicz, and A. Winguth, Future ocean uptake of CO₂: interaction between ocean circulation and biology, *Clim. Dyn.*, 12, 711–721, 1996.
- Maqueda, M. M., and S. Rahmstorf, Did Antarctic sea-ice expansion cause glacial CO₂ decline?, *Geophys. Res. Lett.*, 29, 41–43, 2002.
- Marino, B. D., M. B. McElroy, R. J. Salawitch, and W. G. Spaulding, Glacial-to-interglacial variations in the carbon isotopic composition of atmospheric CO₂, *Nature*, 357, 461–466, 1992.
- Martin, J. H., Glacial-interglacial CO₂ change: The iron hypothesis, *Paleoceanography*, 5, 1–13, 1990.
- Maslin, M. A., J. Adams, E. Thomas, H. Faure, and R. Haineyoung, Estimating the carbon transfer between the ocean,

- atmosphere and the terrestrial biosphere since the last glacial maximum, *Terra Nova*, 7, 358–366, 1995.
- Mayewski, P. A., et al., Climate Change During the Last Deglaciation in Antarctica, *Science*, 272, 1636–1638, 1996.
- Melillo, J. M., et al., Terrestrial biotic responses to environmental change and feedbacks to climate, in *Climate Change 1995: The Science of Climate Change*, edited by J. T. Houghton et al., pp. 449–481, Cambridge Univ. Press, New York, 1996.
- Milliman, J. D., Production and accumulation of calcium carbonate in the ocean: Budget of a nonsteady state, *Global Biogeochem. Cycles*, 7, 927–957, 1993.
- Monnin, E., A. Indermühle, A. Dällenbach, J. Flückiger, B. Stauffer, T. F. Stocker, D. Raynaud, and J.-M. Barnola, Atmospheric CO₂ concentrations over the last glacial termination, *Science*, 291, 112–114, 2001.
- Mook, W. G., J. C. Bommerson, and W. H. Staverman, Carbon isotope fractionation between dissolved bicarbonate and gaseous carbon dioxide, *Earth Planetary Sci. Lett.*, 22, 169–176, 1974.
- Peltier, W. R., Ice age paleotopography, *Science*, 265, 195–201, 1994.
- Petit, J. R., L. Mounier, J. Jouzel, Y. Korotkevitch, V. Kotlyakov, and C. Lorius, Paleoclimatological implications of the Vostok core dust record, *Nature*, 343, 56–58, 1990.
- Petoukhov, V., A. Ganopolski, M. Claussen, A. Eliseev, C. Kubatzki, and S. Rahmstorf, CLIMBER-2: A climate system model of intermediate complexity, Part I, Model description and performance for present climate, *Clim. Dyn.*, 16, 1–17, 2000.
- Prentice, I. C., M. T. Sykes, M. Lautenschlager, S. P. Harrison, O. Denissenko, and P. J. Bartlein, Modelling the increase in terrestrial carbon storage after the last glacial maximum, *Global Ecol. Biogeography Lett.*, 3, 67–76, 1994.
- Rau, G. H., T. Takahashi, and D. J. D. Marais, Latitudinal variations in planktonic $\delta^{13}\text{C}$: Implications for CO₂ and productivity in past oceans, *Nature*, 341, 516–518, 1989.
- Schulz, M., D. Seidov, M. Sarnthein, and K. Stattegger, Modeling ocean-atmosphere carbon budgets during the Last Glacial Maximum—Heinrich 1 meltwater event—Bølling transition, *Int. J. Earth Sci. (Geol. Rundsch)*, 90, 412–415, 2001.
- Shackleton, N. J., Carbon-13 in *Uvigerina*: Tropical rainforest history and the equatorial Pacific carbonate dissolution cycles, in *The Fate of Fossil Fuel CO₂ in the Oceans*, edited by N. R. Andersen and A. Malahoff, pp. 401–428, Plenum, New York, 1977.
- Shaffer, G., A non-linear climate oscillator controlled by biogeochemical cycling in the ocean: an alternative model of Quaternary ice age cycles, *Clim. Dyn.*, 4, 127–143, 1990.
- Siegenthaler, U., and K. O. Münnich, ¹³C/¹²C fractionation during CO₂ transfer from air to sea, In *Carbon Cycle Modelling*, edited by B. Bolin, pp. 249–257, John Wiley, New York, 1981.
- Sigman, D. M., and E. A. Boyle, Glacial/interglacial variations in atmospheric carbon dioxide, *Nature*, 407, 859–869, 2000.
- Sigman, D. M., D. C. McCorkle, and W. R. Martin, The calcite lysocline as a constraint on glacial/interglacial low-latitude production changes, *Global Biogeochem. Cycles*, 12, 409–427, 1998.
- Six, K. D., and E. Maier-Reimer, Effects of plankton dynamics on seasonal carbon fluxes in an ocean general circulation model, *Global Biogeochem. Cycles*, 10, 559–583, 1996.
- Smetacek, V., EisenEx: International team conducts iron experiment in the Southern Ocean, *U.S. JGOFS Newsletter*, 11, 11–14, 2001.
- Smith, H. J., H. Fischer, M. Wahlen, D. Mastroianni, and B. Deck, Dual modes of the carbon cycle since the Last Glacial Maximum, *Nature*, 400, 248–250, 1999.
- Stephens, B. B., and R. F. Keeling, The influence of Antarctic sea ice on glacial-interglacial CO₂ variations, *Nature*, 404, 171–174, 2000.
- Tans, P. P., J. A. Berry, and R. F. Keeling, Oceanic ¹³C/¹²C observations: a new window on ocean CO₂ uptake, *Glob. Biogeochem. Cycles*, 7, 353–368, 1993.
- Treguer, P., and P. Pondaven, Global change: Silica control of carbon dioxide, *Nature*, 406, 358–359, 2000.
- Volk, T., and M. I. Hoffert, Ocean carbon pumps: Analysis of relative strengths and efficiencies in ocean-driven atmospheric CO₂ changes, in *The Carbon Cycle and Atmospheric CO₂: Natural Variations Archean to Present*, *Geophys. Monogr. Ser.*, vol. 32, edited by E. T. Sunquist and W. S. Broecker, pp. 99–110, AGU, Washington, D. C., 1985.
- Watson, A. J., D. C. E. Bakker, A. J. Ridgwell, P. W. Boyd, and C. S. Law, Effect of iron supply on Southern Ocean CO₂ uptake and implications for glacial atmospheric CO₂, *Nature*, 407, 730–733, 2000.
- Zhang, J., P. D. Quay, and D. O. Wilbur, Carbon isotope fractionation during gas-water exchange and dissolution of CO₂, *Geochim. Cosmochim. Acta*, 59, 107–114, 1995.